Band-filling and magnetic-field effects on the phase diagram of one-dimensional conductors

G. Montambaux, M. Héritier, and P. Lederer
Laboratoire de Physique des Solides, Bâtiment 510, Université Paris-Sud, 91405 Orsay, France
(Received 15 July 1985)

We investigate the Fermi gas model for one-dimensional (1D) conductors as a function of chemical potential and of the applied magnetic field. The bosonization method allows to prove the equivalence between these parameters, the first acting on charge degrees of freedom, the second on spin degrees of freedom. A number of results available in the literature can thus be connected. We also use the mapping to the 2D classical Coulomb gas and a two-cutoff renormalization-group method, the two energy scales being the bandwidth and the Zeeman energy (or the chemical potential). We obtain a coherent description of the Fermi gas phase diagram as a function of these two "fields."

I. INTRODUCTION

In the rapid development of research on organic quasi-one-dimensional systems, experimental results on the phase diagram of these compounds in a magnetic field has sparked theoretical activity.[1] It is well recognized that the spectacular effects observed in the tetramethyltetraselenafulvalene family [$(TMTSF)_2X$] namely, the occurrence of a cascade of field-induced spin-density-wave (SDW) phases, are due to magnetic orbital effects.[2] However, it is interesting to study spin effects of the magnetic field in a strictly one-dimensional (1D) electron gas for various reasons: under a suitable field geometry, orbital effects can be made small, and one can think of systems with small enough transverse coupling $t_\perp$ between 1D chains such that in a suitable temperature range and large enough magnetic fields, the quasi-1D crystal behaves electronically as a collection of independent 1D chains. Such metals should be considered as quasi-1D conductors in which large quantum or thermal fluctuations strongly influence all the physical properties down to some low-temperature 1D-3D crossover. Given the interest in this domain and constant efforts to synthesize new compounds in which more or less pronounced 1D character could be revealed, it appears necessary to perform a complete investigation of the 1D electron gas in a magnetic field. This study only deals with spin effects since there is no orbital effect in a strictly 1D system. This study relates very closely to the problem of the behavior of the 1D electron gas as a function of the band filling or the chemical potential. In a number of real compounds, such as, e.g., in the $(TMTSF)_2X$ family, umklapp processes arise because of a complete electronic transfer and a dimerization which leaves a half-filled band. These processes are thought to be essential to the understanding of these compounds.[3,4] On the other hand, a number of synthetic organic metals exhibit a continuous variation of charge transfer as a function of temperature, pressure, etc., whence the importance of studying the approach to commensurability. Moreover, one can think of experiments in which the band filling or chemical potential as well as the magnetic field can be varied together, whence the purpose of this paper is to investigate the behavior of the 1D electron gas as a function of these two "fields." The intent of such a study is to allow better predictions of actual 3D (three-dimensional) ordered phases under various external fields.

We use a model in which electron-electron interactions are reduced to scattering processes between electrons close to the Fermi surface.[5,6] Each process is characterized by a constant g_i: this is the so-called "g-ology" model (hereafter referred to as the constant-g_i model). The electrons interact through backward scattering with coupling strength g_1 (momentum transfer $q \simeq 2k_F$) and forward scattering with coupling g_2 ($q \simeq 0$). We emphasize the spin dependence of the backward-scattering processes since the $g_{1\perp}$ processes between electrons of opposite spins are inhibited by the magnetic field.[7] We also consider an umklapp scattering g_3 which is important in the case of a half-filled band. The g_3 processes are inhibited by deviation from the half-filled band. This effect has been studied by Seidel and Prigodin,[8,9] using a renormalization-group (RG) technique. We have used a similar procedure to investigate the magnetic-field effects in 1D and quasi-1D electron gases.[7] In the case of an attractive interaction $g_{1\parallel} < 0$, Japaridze and Nersesyan[10] studied the electron gas in a field, using the bosonization method and the exact Luther-Emery solution.[11] In those papers, magnetic field and band-filling effects were never studied together. One of the goals of this paper is to take advantage of the analogy between these "fields" to treat them as well as their combined effects in close analogy.

Emery *et al.*[12] have already shown that umklapp scattering has the same effect on the charge degrees of freedom as backward scattering ($g_{1\perp}$) has on the spin degrees of freedom. However, they set up this equivalence only in the case of a half-filled band and pointed out that a difference occurs when $4k_F$ is not a vector of the reciprocal lattice, $G \neq 4k_F$.

The equivalence also holds in that case, if a magnetic field is applied to the electron gas: this field has, on the spin degrees of freedom, exactly the same effect which the

chemical potential has on the charge part of the Hamiltonian. It allows us to describe in a very symmetric way band-filling and field effects. This is shown in Sec. V.

In Sec. VI, we use the mapping of this 1D electron-gas model on the two-dimensional (2D) classical models such as the Coulomb gas, and a RG treatment under magnetic field (or incommensurability). Then, we derive the exponents of response functions and deduce a complete description of the 1D electron gas as a function of these two "fields." The usefulness of this description for the understanding of actual quasi-1D systems is briefly discussed in the conclusion.

II. THE MODEL

Interactions between electrons are described through elementary scattering processes connecting electron states close to the Fermi sea.[5] The appropriate Hamiltonian is $H=H_0+H_{\rm int}+H_z$. In the unperturbed part H_0, the kinetic energy has been linearized so that

$$H_0=v_F\sum_{k,s}k(a_{ks}^\dagger a_{ks}-b_{ks}^\dagger b_{ks})\ , \tag{2.1}$$

where creation operators have been introduced for the right- and left-going branches of the Fermi sea ($a_k^\dagger$ and $b_k^\dagger$). s is a spin index. The interaction term is written as

$$\begin{aligned}H_{\rm int}=&g_2\int\psi_{2s}^\dagger\psi_{2s}\psi_{1s'}^\dagger\psi_{1s'}dx\\&+(g_{1\parallel}\delta_{ss'}+g_{1\perp}\delta_{s,-s'})\int\psi_{1s}^\dagger\psi_{2s}\psi_{2s'}^\dagger\psi_{1s'}dx\\&+g_3\int(\psi_{1s}^\dagger\psi_{2s}\psi_{1,-s}^\dagger\psi_{2,-s}e^{-iGx}+\text{H.c.})dx\ ,\end{aligned} \tag{2.2}$$

where

$$\psi_{1s}(x)=L^{-1/2}\sum_k e^{ikx}a_{ks}\ ,$$

$$\psi_{2s}(x)=L^{-1/2}\sum_k e^{ikx}b_{ks}\ .$$

The sums over s and s' are implicit.

As will be seen below, the backward scattering $g_{1\perp}$ between electrons of opposite spins is strongly affected by the magnetic field so that we have chosen to distinguish the two processes $g_{1\parallel}$ and $g_{1\perp}$. Because of the Pauli exclusion principle, the umklapp term g_3 couples only electrons with opposite spins. A detailed review on this Hamiltonian in zero magnetic field, either in the case $G=4k_F$ for a half-filled band or when $g_3=0$ is given by Solyom.[5] H_z is the Zeeman coupling to the field:

$$H_z=\mu_B H\sum_{k,s}s(a_{ks}^\dagger a_{ks}+b_{ks}^\dagger b_{ks}),\quad s=\pm1 \tag{2.3}$$

which splits the energy spectrum of H_0 into two subbands of opposite spins. In the following we note $h=\mu_B H$.

III. PERTURBATION EXPANSION

It is expected that the magnetic field and the deviation from the $G=4k_F$ commensurability inhibit certain scattering processes. This can be seen in a diagrammatic expansion of the vertex function which now involves scattering of electrons away from the Fermi surface.[5]

To lowest order, one obtains for the real contribution to the vertices

$$\Gamma_{\parallel}-\Gamma_{2\perp}=\bar g_{1\parallel}+\bar g_{1\perp}^2\ln\left[\frac{|\omega^2-16h^2|^{1/2}}{E_0}\right]+\cdots\ , \tag{3.1a}$$

$$\Gamma_{1\perp}=\bar g_{1\perp}+\tfrac12\bar g_{1\perp}\bar g_{1\parallel}\times\left[\ln\left[\frac{\omega}{E_0}\right]+\ln\left[\frac{|\omega^2-16h^2|^{1/2}}{E_0}\right]\right]+\cdots\ , \tag{3.1b}$$

$$\Gamma_{\parallel}+\Gamma_{2\perp}=\bar g_{1\parallel}-2\bar g_2+\bar g_3^2\ln\left[\frac{|\omega^2-16\delta\mu^2|^{1/2}}{E_0}\right]+\cdots\ , \tag{3.2a}$$

$$\Gamma_3=\bar g_3+\tfrac12\bar g_3(\bar g_{1\parallel}-2\bar g_2)\times\left[\ln\left[\frac{\omega}{E_0}\right]+\ln\left[\frac{|\omega^2-16\delta\mu^2|^{1/2}}{E_0}\right]\right]+\cdots\ , \tag{3.2b}$$

where $\bar g_i=g_i/\pi v_F$ and $\delta\mu=v_F(k_F-G/4)$. E_0 is a bandwidth cutoff. We have mixed the appropriate vertex functions in order to display the well-known decoupling between the $(g_{1\parallel},g_{1\perp})$ and $(g_{1\parallel}-2g_2,g_3)$ sets of parameters, corresponding, respectively, to spin and charge degrees of freedom. Then it is already obvious that the incommensurability acts on the charge degrees of freedom, exactly as the magnetic field acts on the spin degrees of freedom, the first inhibiting the $g_{1\perp}$ processes, the second affecting the umklapp processes.

IV. RENORMALIZATION-GROUP TREATMENT

We consider, for example, the space $(g_{1\parallel},g_{1\perp})$ involved in perturbation expansions (3.1a) and (3.1b). From these expansions we use a renormalization procedure which connects properties of the model with different cutoff energies. Here, due to the presence of two energy scales E_0 and h, the renormalization is twofold.[7]

In the first regime, the cutoff energy parameter is larger than the field so that the field effect is neglected and one first performs a zero-field renormalization. In the second regime, when the cutoff parameter is smaller than the field, backward scattering is supposed to be totally frozen. This amounts to replacing $\ln(|\omega^2-16h^2|^{1/2}/E_0)$ either by $\ln(\omega/E_0)$ (first regime) or by 0 (second regime). This leads to the following Lie equations, to lowest order $[l=\ln(E_0'/E_0)]$:

$$\frac{d\bar g_{1\parallel}}{dl}=\bar g_{1\perp}^2,\quad \frac{d\bar g_{1\perp}}{dl}=\bar g_{1\parallel}\bar g_{1\perp}\ \text{ when }\ E_0'\gtrsim4h\ , \tag{4.1a}$$

$$\frac{d\bar g_{1\parallel}}{dl}=0,\quad \frac{d\bar g_{1\perp}}{dl}=\tfrac12\bar g_{1\parallel}\bar g_{1\perp}\ \text{ when }\ E_0'\lesssim4h\ . \tag{4.1b}$$

The essential effect of the field is to stop the renormalization of $g_{1\parallel}$ when $E_0'\approx4h$. Moreover, since $g_{1\perp}$ process-

es are inhibited by the field, it can be shown that $g_{1\perp}$ does not appear in the low-frequency response functions under the field[7,9] so that the only effect of $g_{1\perp}$ (g_3) is a renormalization of $g_{1\parallel}$ ($g_{1\parallel}-2g_2$) in the exponents of the response functions.

Equations (4.1) are the simplest equations which describe the renormalization trajectories in the field. They provide essential results, namely, the separation between a weak-coupling region $g_{1\parallel}\geq|g_{1\perp}|$ with a line of fixed points $g^*_{1\perp}=0$ (Tomonaga-like behavior), and a strong-coupling region characterized by a gap.[5] The study of the field effect[7] leads to results identical to those deduced from a "parquet" treatment.[13] Indeed, that method is known to be equivalent to a first-order renormalization. Here, for the sake of simplicity, we have limited ourselves to this first order. But the physics that we describe has been studied using a second-order scaling method without the above simplification of logarithmic terms.[8] The calculation must be performed numerically and leads qualitatively to the same results, namely that, when the energy scale is smaller than the Zeeman energy, the inhibition of the $g_{1\perp}$ process stops the renormalization of $g_{1\parallel}$. Later in this paper, we will apply that result in particular to the study of the strong-coupling region by going beyond first-order scaling. Thus, using the renormalization-group treatment, critical exponents will be estimated as a function of the field. In the following section, we first turn to the use of the bosonization method.

V. BOSON REPRESENTATION

The interest of this method is manifold. It allows us to decouple spin and charge degrees of freedom and thus to prove the equivalence between magnetic-field and band-filling effects. It yields an exact solution in the strong-coupling region. It maps the electron-gas problem on to 2D classical models such as the Coulomb gas for which RG equations are better known and provide a better understanding of the strong-coupling region.

The Hamiltonian of Sec. II can be expressed in terms of density operators

$$\rho_{rs}(x)=\psi^\dagger_{rs}\psi_{rs}\ , \tag{5.1}$$

where $r=1,2$ is the band index and $s=\pm1$. The boson representation of the fermion field operator is

$$\psi_{rs}(x)=\frac{1}{\sqrt{2\pi\alpha}}e^{-i\phi_{rs}(x)} \tag{5.2}$$

with

$$\phi_{rs}(x)=2\pi(-1)^{r+1}\int\rho_{rs}(x)dx\ , \tag{5.3}$$

α is an appropriate cutoff, the inverse of the bandwidth cutoff (see the discussion in Ref. 5). The density operators obey bosonlike commutation relations

$$[\rho_{rs}(x),\phi_{r's'}(x')]=i\delta(x-x')\delta_{rr'}\delta_{ss'}\ . \tag{5.4}$$

When the charge and spin-density operators are defined[14]

$$\begin{aligned}&\rho_r(x)=\frac{1}{\sqrt2}(\rho_{r\uparrow}+\rho_{r\downarrow}),\quad \phi^\rho_r(x)=\frac{1}{\sqrt2}(\phi_{r\uparrow}+\phi_{r\downarrow})\ ,\\ &\sigma_r(x)=\frac{1}{\sqrt2}(\rho_{r\uparrow}-\rho_{r\downarrow}),\quad \phi^\sigma_r(x)=\frac{1}{\sqrt2}(\phi_{r\uparrow}-\phi_{r\downarrow})\ ,\end{aligned} \tag{5.5}$$

the Hamiltonian splits into two parts describing spin and charge degrees freedom:[11]

$$\begin{aligned}H_\sigma=&\pi v_F\int(\sigma_1\sigma_1+\sigma_2\sigma_2)dx-g_{1\parallel}\int\sigma_1\sigma_2dx\\&+\frac{2g_{1\perp}}{(2\pi\alpha)^2}\int\cos[\sqrt2(\phi^\sigma_1-\phi^\sigma_2)]dx\\&+h\sqrt2\int(\sigma_1+\sigma_2)dx\ ,\end{aligned} \tag{5.6}$$

$$\begin{aligned}H_\rho=&\pi v_F\int(\rho_1\rho_1+\rho_2\rho_2)dx-(g_{1\parallel}-2g_2)\int\rho_1\rho_2dx\\&+\frac{2g_3}{(2\pi\alpha)^2}\int\cos[\sqrt2(\phi^\rho_1-\phi^\rho_2)-Gx]\\&-\sqrt2v_Fk_F\int(\rho_1+\rho_2)dx\ .\end{aligned} \tag{5.7}$$

This constitutes the so-called boson representation of the Hamiltonian of Sec. II.[12] This decoupling clearly displays the correspondence $(g_{1\parallel}-2g_2,g_3)\leftrightarrow(g_{1\parallel},g_{1\perp})$. We discuss now field and band-filling effects.

Introducing the canonical variables

$$\begin{aligned}&\phi_\nu(x)=\frac{\phi^\nu_1-\phi^\nu_2}{\sqrt{4\pi}}=\sqrt\pi\int(\nu_1+\nu_2)dx,\quad \nu=\rho\text{ or }\sigma\\&\Pi_\nu(x)=\sqrt\pi(\nu_1-\nu_2),\quad \nu=\rho\text{ or }\sigma\end{aligned} \tag{5.8}$$

each part of the Hamiltonian can be reduced to the sine-Gordon form

$$\begin{aligned}H_\sigma=v_F\int\Bigg[&\left[1+\frac{\bar g_{1\parallel}}{2}\right]\frac{\Pi^2_\sigma}{2}+\left[1-\frac{\bar g_{1\parallel}}{2}\right]\frac{\nabla\phi^2_\sigma}{2}\\&+\frac{2g_{1\perp}}{(2\pi\alpha)^2}\cos(\sqrt{8\pi}\phi_\sigma)+h\left[\frac{2}{\pi}\right]^{1/2}\nabla\phi_\sigma\Bigg]dx\ ,\end{aligned} \tag{5.9}$$

$$\begin{aligned}H_\rho=v_F\int\Bigg[&\left[1+\frac{\bar g_\rho}{2}\right]\frac{\Pi^2_\rho}{2}+\left[1-\frac{\bar g_\rho}{2}\right]\frac{\nabla\phi^2_\rho}{2}\\&+\frac{2g_3}{(2\pi\alpha)^2}\cos(\sqrt{8\pi}\phi_\rho-Gx)\\&-\mu\left[\frac{2}{\pi}\right]^{1/2}\nabla\phi_\rho\Bigg]dx\ ,\end{aligned} \tag{5.10}$$

where $\bar g_\rho=\bar g_{1\parallel}-2\bar g_2$. μ is the chemical potential of the interacting electron gas. The two Hamiltonians are exactly identical provided a new choice of the phase:

$$\phi'_\rho=\phi_\rho-\frac{G}{\sqrt{8\pi}}x\ . \tag{5.11}$$

This phase shift amounts to taking the origin of the density at the half-filled band. The forms (5.9) and (5.10)

TABLE I. Equivalence obtained by inversion of charge and spin degrees of freedom.

Charge degrees of freedom	Spin degrees of freedom
$\delta\mu$, chemical potential	h, magnetic field
$g_{1\parallel}-2g_2$	$g_{1\parallel}$
g_3	$g_{1\perp}$
CDW	CDW
SDW	SS
SS	SDW
TS	TS
n, electron density	m, magnetization

display the exact correspondence between the effect of the field on the spin degrees of freedom and that of the chemical potential on the charge degrees of freedom (see Table I). Then strong analogies can be developed for the 1D electron gas in a magnetic field or as a function of the band filling, as was already stressed from the perturbative expansion. The gradient term in each Hamiltonian is either the coupling of the magnetization $m=(2/\pi)^{1/2}\int\nabla\phi_\sigma dx$ to the magnetic field, or the coupling of the electron density $n=(2/\pi)^{1/2}\int\nabla\phi_\rho dx$ to the chemical potential.

Hamiltonians of the form (5.9) and (5.10) have already been extensively discussed in the literature. They are well known to be equivalent to a classical 2D sine-Gordon functional with incommensurability along one direction, the magnetization and the electron density being equivalent to the mean incommensurability or the soliton density of the sine-Gordon problem.[15,16] For this Hamiltonian, RG equations have been derived directly[16] and give equivalent results to those obtained in the constant-g_i model.[7,9] In the sine-Gordon problem, the behavior of the renormalization flow changes when the lattice scaling parameter reaches the soliton separation. At this stage, the pinning potential stops contributing to the free energy[16] exactly as the $g_{1\perp}$ processes are inhibited when the energy scaling parameter is of order of the field.

Finally, it is known that H_σ or H_ρ can be transformed into a 1D interacting spinless-fermion (SF) model, using the boson representation of a spinless-fermion operator. In the particular case where $\bar{g}_{1\parallel}=-\frac{6}{5}$ (or $\bar{g}_{1\parallel}-2\bar{g}_2=-\frac{6}{5}$) the SF's are free so that there exists an exact solution for this coupling which has been found by Luther and Emery[11] (LE). Applying a field to H_σ or a chemical potential to H_ρ amounts to changing the Fermi level of the SF. In this picture, it is known that there is no change in the ground-state properties as long as the SF Fermi level lies in the gap, namely, when $h<h_c=\Delta_\sigma$ (or $\delta\mu<\Delta_\rho$) where Δ is the renormalized value of the gap of the spin (or charge) excitations. $\Delta_\sigma=g_{1\perp}/2\pi\alpha$ (or $\Delta_\rho=g_3/2\pi\alpha$) on the LE line and $\Delta=0$ in the low coupling region $g_{1\parallel}\geq|g_{1\perp}|$ (or $g_{1\parallel}-2g_2\geq|g_3|$).

The magnetization and the density are related to the SF density of states at the Fermi level.[10] When there is no gap, the magnetization varies as $m=2h/\pi v_\sigma$ and the electron density as $n=2\mu/\pi v_\rho$ where v_σ and v_ρ are Fermi velocity renormalized by parallel interactions: $v_\sigma=v_F(1-\bar{g}_{1\parallel}/2)^{-1}$ and $v_\rho=v_F(1-\bar{g}_\rho/2)^{-1}$. In the strong-coupling region

$$m=0 \text{ when } h<h_c\ ,$$
$$m=\frac{2}{\pi v_\sigma}(h^2-h_c^2)^{1/2}\mathrm{sgn}(h) \text{ when } h>h_c\ , \tag{5.12}$$

$$n=G/2\pi \text{ when } \delta\mu<\delta\mu_c\ ,$$
$$n=G/2\pi+\frac{2\,\mathrm{sgn}(\delta\mu)}{\pi v_\rho}(\delta\mu^2-\delta\mu_c^2)^{1/2} \text{ when } \delta\mu>\delta\mu_c\ , \tag{5.13}$$

where $\delta\mu$ is such that $n=G/2\pi$ when $\delta\mu=0$.

The Fermi wave vector k_F in presence of interactions is given by $\tilde{k}_F=(\pi/2)n$ so that $\tilde{k}_F=G/4$ as soon as $\delta\mu<\delta\mu_c$ and $\tilde{k}_F-G/4\propto(\delta\mu^2-\delta\mu_c^2)^{1/2}$ when $\delta\mu>\delta\mu_c$.[15] In the presence of a field, there are two subbands of opposite spin with Fermi wave vectors:

$$\tilde{k}_{F,s}=\tilde{k}_F+\frac{s}{v_\sigma}(h^2-h_c^2)^{1/2}\ . \tag{5.14}$$

At $T=0$, the susceptibility[10] varies as

$$\chi=\frac{1}{\pi v_\sigma}\frac{h}{(h^2-h_c^2)^{1/2}},\quad h>h_c\ . \tag{5.15}$$

Similarly, there is a divergence of the compressibility in the case of a non-half-filled band:

$$\kappa\propto\frac{1}{(\delta\mu^2-\delta\mu_c^2)^{1/2}},\quad \delta\mu>\delta\mu_c\ . \tag{5.16}$$

Because of the gap in the H spectrum, Emery *et al.*[12] found for the magnetic susceptibility an activated behavior at finite temperature:

$$\chi=\frac{1}{\pi v_\sigma}(2\pi\beta\Delta)^{1/2}e^{-\beta\Delta} \tag{5.17}$$

and the compressibility exhibits also such a behavior when there is a gap in the H_ρ spectrum.

The behavior of the magnetic susceptibility and of the specific heat at finite temperature and for different limits has been discussed in the presence of a field.[10] Similar behaviors are thus expected as functions of the band filling, namely, an activated dependence of the compressibility and of the charge part of the specific heat C_ρ when $\delta\mu<\delta\mu_c$, the activation energy of which increases towards its half-filled-band value; a divergence of the compressibility when $\delta\mu=\delta\mu_c$; a specific-heat crossover from an activated behavior when $\delta\mu<\delta\mu_c$ to a linear temperature dependence when $\delta\mu>\delta\mu_c$. At $\delta\mu=\delta\mu_c$, C_ρ varies as $\sqrt{T}$.

VI. RESPONSE FUNCTIONS

We now explore the behavior of the different instabilities in a field (h or $\delta\mu$). We know from the preceding section that the wave vector of each instability (CDW denotes a charge-density wave, SDW a spin-density wave, SS singlet superconductivity, and TS triplet superconductivity) is connected to the density and the magnetization of the electron gas

$$
\begin{aligned}
&Q_{\mathrm{CDW}}=\pi(n\pm m)\ ,\\
&Q_{\mathrm{SDW}}=\pi n\ ,\\
&Q_{\mathrm{SS}}=\pm\pi m\ ,\\
&Q_{\mathrm{TS}}=0\ ,
\end{aligned}
\tag{6.1}
$$

with expressions of n and m given above. Now, we recall the multiplicative structure of the response functions, due to the separation of spin and charge degrees of freedom:[6]

$$
\begin{aligned}
&N(x,t)\propto S_\rho^+(x,t)S_\sigma^+(x,t)\ \text{ for CDW}\ ,\\
&\chi(x,t)\propto S_\rho^+(x,t)S_\sigma^-(x,t)\ \text{ for SDW}\ ,\\
&\Delta_s(x,t)\propto S_\rho^-(x,t)S_\sigma^+(x,t)\ \text{ for SS}\ ,\\
&\Delta_t(x,t)\propto S_\rho^-(x,t)S_\sigma^-(x,t)\ \text{ for TS}\ .
\end{aligned}
\tag{6.2}
$$

Δ_s (Δ_t) defines the response functions appropriate to the singlet (triplet) superconductivity. The functions $S_\rho^\pm$ ($S_\sigma^\pm$) are the contribution of the charge (spin) degrees of freedom and have been calculated independently from each part of the Hamiltonian.[17–19]

From this structure and the previous considerations, the Table I of equivalences can be derived, resulting from a permutation of charge and spin degrees of freedom. The behavior of response functions under a magnetic field is the same as with $\delta\mu\neq 0$ provided charge and spin degrees of freedom have been inverted. For example, the field h acts on the SDW instability exactly as $\delta\mu$ acts on the SS one. Taking advantage of this parallelism, we now explore the different parts of the phase diagram. The effect of the chemical potential has been studied by Seidel and Prigodin.[8,9] Japaridze and Nersesyan[10] looked at the electron gas with an attractive interaction ($g_{1\|}<0$) under a field around the LE line. We have discussed the effect of the field h in the weak-coupling region ($g_{1\|}\geq|g_{1\perp}|$) and when $g_{1\|}>0$ (regions A and B of Fig. 1).[7] Although much work has been performed on this subject, we give here for the first time a complete discussion of the phase diagram under fields, with emphasis on the combined effect of h and $\delta\mu$. In the following, exponents γ_ρ and γ_σ are defined as

$$
\begin{aligned}
&S_\rho^\pm(x)\propto x^{-\gamma_\rho^{\pm1}}\ ,\\
&S_\sigma^\pm(x)\propto x^{-\gamma_\sigma^{\pm1}}\ .
\end{aligned}
\tag{6.3}
$$

We now investigate the different parts of the phase diagram.

A. $g_{1\|}\geq|g_{1\perp}|$, $g_{1\|}-2g_2\geq|g_3|$

We first discuss the problem when $h=0$ and $\delta\mu=0$. There is no gap in any part of the Hamiltonian. The problem scales to the Tomonaga solution so that all response functions exhibit a power law divergence ω^μ (Ref. 20)

$$
\mu=\begin{cases}
\gamma_\rho+\gamma_\sigma-2 & \text{for CDW},\\
\gamma_\rho+1/\gamma_\sigma-2 & \text{for SDW},\\
1/\gamma_\rho+\gamma_\sigma-2 & \text{for SS},\\
1/\gamma_\rho+1/\gamma_\sigma-2 & \text{for ST}\ ,
\end{cases}
\tag{6.4}
$$

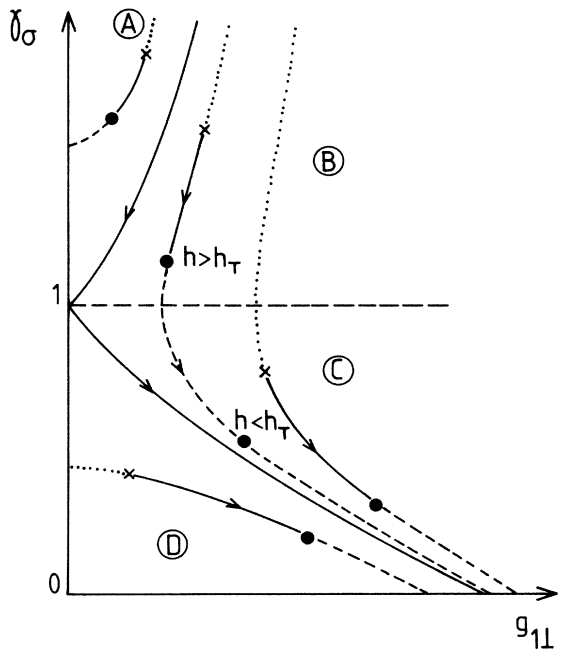

FIG. 1. Renormalization trajectories in the $(\gamma_\sigma,g_{1\perp})$ plane for different values of the magnetic field. A similar result is obtained for the (γ_ρ,g_3) plane as function of the chemical potential. Four regions are separated by the thick curve and by the line $\gamma_\sigma=1$. The bare coupling indicated with a cross is the starting point of the renormalization which stops when the energy scale is equal to the field. Dashed curves are the trajectories when the field is zero (region A) or smaller than the gap h_c (regions B, C, and D). When the starting point lies in region B, there is a critical field h_T above which the renormalized exponent γ_σ becomes larger than 1. Dotted curves are continuations of the trajectories.

where

$$
\gamma_\sigma=\left[\frac{1+\bar g_{1\|}^*/2}{1-\bar g_{1\|}^*/2}\right]^{1/2},\quad \gamma_\rho=\left[\frac{1+(\bar g_{1\|}^*-2\bar g_2^*)/2}{1-(\bar g_{1\|}^*-2\bar g_2^*)/2}\right]^{1/2},
\tag{6.5}
$$

g_i^* are the fixed-point values of the renormalized processes. From a first-order renormalization which is known to be a good approximation in this region:

$$
\begin{aligned}
&g_{1\|}^*=(g_{1\|}^2-g_{1\perp}^2)^{1/2},\ g_{1\perp}^*=0\ ,\\
&g_{1\|}^*-2g_2^*=[(g_{1\|}-2g_2)^2-g_3^2]^{1/2},\ g_3^*=0\ .
\end{aligned}
\tag{6.6}
$$

Since γ_ρ and γ_σ are greater than unity ($\gamma_\sigma=1$ in the spin-independent coupling case $g_{1\|}=g_{1\perp}$), the CDW response is not singular. The dominant singularity is the TS response. SS and SDW responses can be also divergent with a lower degree of divergence. The magnetic field leaves γ_ρ unchanged while, under field, the fixed point is moved to the value

$$
g_{1\|}^*(h)=g_{1\|}^*\frac{1+\dfrac{g_{1\|}-g_1^*}{g_{1\|}+g_1^*}\left[\dfrac{4h}{E_0}\right]^{2g_{1\|}^*}}{1-\dfrac{g_{1\|}-g_1^*}{g_{1\|}+g_1^*}\left[\dfrac{4h}{E_0}\right]^{2g_{1\|}^*}},\quad g_{1\perp}^*(h)=0
\tag{6.7}
$$

with $g_1^*=g_{1\|}^*(h=0)$. In the case of spin-independent coupling $g_{1\|}=g_{1\perp}=g_1$,

$$g_1^*(h)=\frac{g_1}{1-\bar{g}_1\ln\frac{4h}{E_0}} . \tag{6.8}$$

In any case, the fixed point is moved to a higher value so that $\gamma_\sigma(h)>\gamma_\sigma(h=0)$. A higher-order renormalization does not alter this behavior.

As a result, the magnetic field effect in this region does not change the main singularity which is always TS but the SDW is favored as a secondary divergence at the expense of the SS one. We have shown that the SDW can thus be stabilized in the quasi-1D Fermi gas.[7]

Quite symmetrically, deviation from the commensurability $G=4k_F$ leaves the dominant singularity unchanged but favors the SS fluctuations. When both "fields" (h and $\delta\mu$) are "applied," their effects compensate, one favoring SDW, the other SS instability.

B. $g_{1\|}<|g_{1\perp}|$, $g_{1\|}-2g_2\geq|g_3|$

We concentrate now on the spin part of the Hamiltonian, the ρ part being Tomonaga like as in the previous case ($\gamma_\rho>1$). We enter in the strong-coupling region for H_σ, which is much less known so that our evaluation of the field effect is at best qualitative. In zero field, on the LE line, $S_\sigma^\pm$ can be expressed in terms of the SF correlation functions.[17–19] When $x\to\infty$, $S_\sigma^+(x)$ is constant and $S_\sigma^-(x)$ decreases exponentially, leading to an exponential disappearance of the TS and SDW correlations. This means that the exponent γ_σ is now 0. More generally, when $g_{1\|}<|g_{1\perp}|$, there is a gap in the σ part of the excitation spectrum so that $\gamma_\sigma=0$. The important point is that, when no magnetic field is applied, either $\gamma_\sigma>1$ in the low-coupling Tomonaga-like region described above or $\gamma_\sigma=0$ in the strong-coupling region. The region in phase space such that $0<\gamma_\sigma<1$ is forbidden in zero field (Figs. 1 and 2). The main effect of the field is to make part of it accessible. From Sec. V, we know that the behavior of the Fermi gas is unchanged as long as the magnetic field is smaller than the gap, $h<h_c=\Delta_\sigma$. We are now facing two problems. One is to know or at least estimate the value of the gap in the whole strong-coupling region, away from the LE line where it is known exactly. The second is to find the behavior of the response functions when $h>\Delta_\sigma$.

It is well known that the first-order RG equations do not provide a good description of the strong-coupling region. A better choice is the use of the RG equations for the Coulomb gas which has been demonstrated to be equivalent to the bosonized form of the constant-g_i problem.[21] Using the following correspondence:[21]

$$\begin{aligned} y &\leftrightarrow \frac{\bar{g}_{1\perp}}{4\pi(1-\bar{g}_{1\|}^2/4)^{1/2}}, \quad \bar{g}_i=g_i/\pi v_F \\ K &\leftrightarrow 4\left[\frac{1+\bar{g}_{1\|}/2}{1-\bar{g}_{1\|}/2}\right]^{1/2}=4\gamma_\sigma , \end{aligned} \tag{6.9}$$

where K is the coupling constant and y the fugacity of the Coulomb gas, one deduces the following RG equations for the parameter space $(\gamma_\sigma, g_{1\perp})$:

$$\frac{d\gamma_\sigma}{dl}=\frac{\bar{g}_{1\perp}^2}{8}(1+\gamma_\sigma^2)^2, \quad \frac{d\bar{g}_{1\perp}}{dl}=2(\gamma_\sigma-1)\bar{g}_{1\perp}, \quad l=\ln\frac{E_0'}{E_0} . \tag{6.10}$$

These equations recover, to lowest order in $g_{1\perp}$ and to next order in $g_{1\|}$, the RG equations found by Solyom[5] directly from the perturbation of the constant-g_i problem. They provide a better estimate of the renormalized couplings in the strong-coupling region and provide directly the renormalized value of the exponent γ_σ of response functions (Fig. 2).

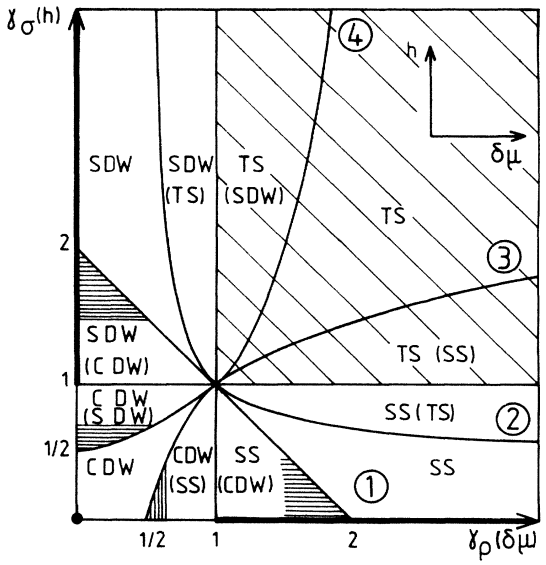

FIG. 2. Phase diagram of the 1D Fermi gas model. The curves 1, 2, 3, and 4 are respectively, defined by $\gamma_\rho+\gamma_\sigma=2$, $\gamma_\rho^{-1}+\gamma_\sigma^{-1}=2$, $\gamma_\rho^{-1}+\gamma_\sigma=2$, and $\gamma_\rho+\gamma_\sigma^{-1}=2$. The "fields" h and $\delta\mu$ move the representative point of the system, respectively, to the top and to the right. A complete understanding of the Fermi gas model under fields can be deduced from this diagram.

In the absence of field, the renormalization trajectories flow to the value $\gamma_\sigma=0$. This point is reached by decreasing the energy scale to a finite value which is precisely the excitation gap, expected from the bosonization method. The gap can be estimated from RG equations at least when it is small, i.e., close to the lines $g_{1\perp}=0$ and $g_{1\|}=|g_{1\perp}|$. Close to the line $g_{1\perp}=0$, from Eq. (6.10), one deduces $\Delta/E_0\propto g_{1\perp}^{1/2(1-\gamma_\sigma)}$ as obtained for the first time in a different way by Luther.[22] This recovers the exact solution of LE when $\gamma_\sigma=\frac{1}{2}$ ($\bar{g}_{1\|}=-\frac{6}{5}$) and the classical solution (infinite mass) of the sine-Gordon equation when $\gamma_\sigma=0$ [$\bar{g}_{1\|}^*=-2$, see Eq. (6.5)].[23] Close to the line $g_{1\|}=|g_{1\perp}|$, the gap is given by a Kosterlitz-Thouless-type expression:[24]

$$\Delta\simeq E_0\exp\frac{-C}{(|\bar{g}_{1\perp}|-\bar{g}_{1\|})^{1/2}} \quad \text{with } C=\frac{\pi}{(2\bar{g}_1)^{1/2}} . \tag{6.11}$$

When $g_{1\parallel}=g_{1\perp}<0$ and both are small, an expression has been also derived[12,25] which recovers the exact result of Ovchinnikov[26] for the Hubbard model.

We turn now to the case of an applied field. As shown in the preceding sections, when the energy scale becomes smaller than the field, the renormalization stops at the corresponding value $\gamma_\sigma(h)$. Thus, as long as the field is smaller than the gap (more precisely $h<\Delta_\sigma$, where the gap is $2\Delta_\sigma$), the trajectories still flow to the same value $\gamma_\sigma(h)=0$ and nothing is changed. When the field is larger than $h_c=\Delta_\sigma$, the renormalization is stopped at the energy scale h, the $g_{1\perp}$ processes becoming irrelevant. Their only effect is a renormalization of γ_σ so that we expect at low frequency ($\omega \ll h$), a Tomonaga-like behavior, the exponent of which, $\gamma_\sigma(h)$, is field dependent, leading to a continuous spanning of the parameter space: when the field increases to infinity (or rather to the cutoff E_0), the coupling constants tend to their bare, nonrenormalized values so that $\gamma_\sigma(h)$ reaches its maximum value

$$\gamma_\sigma(\infty)=\left[\frac{1+\bar{g}_{1\parallel}/2}{1-\bar{g}_{1\parallel}/2}\right]^{1/2}=\gamma_\sigma \text{ (nonrenormalized)} . \tag{6.12}$$

This kind of description, first worked out by Seidel and Prigodin in the band-filling problem[8] exhibits qualitative differences with the result of Japaridze and Nersesyan (JN) obtained from the SF representation.[10] The latter (JN) analyzed the LE line and its vicinity where the corresponding SF Hamiltonian contains four-fermion interactions. When $h>h_c$, the spin-density-excitation dispersion law can be linearized around the Fermi level and a new Tomonaga-Luttinger problem is derived. As a result, the response function behavior is unchanged as long as h is lower than h_c, namely, γ_σ remains 0. When $h>h_c$, the functions $S_\sigma^{\pm}(x)$ decrease algebraically: γ_σ jumps discontinuously from 0 to $\frac{1}{2}$ and reaches its Tomonaga value in infinite field. The asymptotic laws they find are valid only when $x \gg v_F(h^2-h_c^2)^{-1/2}$, i.e., $\omega \ll (h^2-h_c^2)^{1/2}$, thus in a vanishingly small domain of frequency when h is just above h_c. We expect that procedure to be well appropriate close to the LE line while the RG treatment provides a correct understanding if the bare coupling values lie in the vicinity of the weak-coupling region, i.e., just below the $g_{1\parallel}=|g_{1\perp}|$ line and probably as long as $g_{1\parallel}>0$. In fact the RG scaling is not adapted to describe the region below the LE line where bound states occur in the gap.[5] A common feature of the two descriptions is that γ_σ reaches its bare value in high field, which means that the $g_{1\perp}$ processes are totally frozen. Moreover, both give a monotonous increasing variation of γ_σ with the field above the LE line. But, in the SF description, below that line, γ_σ decreases from $\frac{1}{2}$ to a smaller value when h goes from h_c to infinity. Thus, there is in this picture a quite different field effect above and below the LE line. However, as discussed by Solyom,[5] one should be cautious on quantitative results obtained from the bosonized Hamiltonian, because of the problems linked with the cutoff procedure inherent to bosonization.

Nevertheless, concerning the occurrence of the possible instabilities as functions of the field, both methods give at least qualitatively the same indications, apart from a small difference in the strong-coupling region below the LE line as will be shown below. It is known that, in most cases, there are two diverging response functions. If one only looks at the relative behavior of the main instabilities (most diverging response function), a detailed knowledge of the strong-coupling region is not useful. The lines separating regions characterized by different main instabilities are defined by $\gamma_\sigma=1$ and $\gamma_\rho=1$. Thus, an interesting consequence for the field effect occurs in the region where $\gamma_\sigma(h=0)=0$ and $\gamma_\sigma(\infty)>1$. This is the case when $0<g_{1\parallel}<|g_{1\perp}|$ (region B of Fig. 1). Then, there is a second critical field h_T defined by $\gamma_\sigma(h_T)=1$: by applying a field larger than h_T, a SS (CDW) ground state becomes a TS (SDW) ground state.[7] Note that, just below the line $g_{1\parallel}=|g_{1\perp}|$ where we expect the RG treatment to be valid, h_T is given by a Kosterlitz-like expression and that $h_T=(h_cE_0)^{1/2}$.[7] If one becomes interested in the secondary singularity, there are several critical fields h_i such that $\gamma_\sigma^{\pm 1}(h_i)+\gamma_\rho^{\pm 1}=2$. Still in this case, the two descriptions provide the same qualitative results except in a small region. The main features are the following. If the bare coupling constant $g_{1\parallel}$ lies above the LE line, γ_σ increases with the field so that different kinds of instabilities occur successively. If $1<\gamma_\rho<2$ ($0<\bar{g}_{1\parallel}-2\bar{g}_2<+\frac{6}{5}$), the succession of six possible sets of instabilities is the following: SS (CDW)$\rightarrow$SS$\rightarrow$SS (TS)$\rightarrow$TS (SS)$\rightarrow$TS$\rightarrow$TS (SDW) (see Fig. 2; the phases noted between parentheses have a lower degree of divergence). In particular, from JN, if $\frac{3}{2}<\gamma_\rho<2$, the secondary instability (CDW) disappears when the field reaches the gap $h=h_c$, since γ_σ jumps to the value $\frac{1}{2}$. If $\gamma_\rho>2$, only four possible behaviors can be found: SS$\rightarrow$SS (TS)$\rightarrow$TS (SS)$\rightarrow$TS. How many instabilities effectively occur depends on the infinite field value of γ_σ, i.e., on the bare value of the coupling constants (Fig. 2).

We turn now to the case where the bare coupling $g_{1\parallel}$ lies below the LE line. The instability remains SS (CDW) whatever the field when $1<\gamma_\rho<\frac{3}{2}$ ($0<\bar{g}_{1\parallel}-2\bar{g}_2<\frac{10}{13}$) and SS when $\gamma_\rho>2$ ($\bar{g}_{1\parallel}-2\bar{g}_2>+\frac{6}{5}$). But from the JN results, a curious feature occurs when $\frac{3}{2}<\gamma_\rho<2$ provided $\gamma_\sigma(h=\infty)<2-\gamma_\rho$ (horizontally-hatched region in Figs. 2 and 3): as long as $h<h_c$, the instability is SS (CDW). It becomes SS when $h>h_c$ and is again SS (CDW) above a field such that $\gamma_\sigma(h)=2-\gamma_\rho$.

The effect of the chemical potential on the charge part is the same as that described in the preceding section. γ_ρ increases with $\delta\mu$. In particular, the different behaviors as a function of the magnetic field described above as a function of γ_ρ, can be found when $\delta\mu$ varies [the accessible region lying between $\gamma_\rho(\delta\mu=0)$ and $\gamma_\rho(\infty)$]. Deviation from the commensurability tends to inhibit SDW and CDW as secondary singularities, favoring only the superconducting response functions.

C. $g_{1\parallel}\geq|g_{1\perp}|$, $g_{1\parallel}-2g_2<|g_3|$

This case is straightforwardly deduced from the discussion of Sec. VI B, with the mapping of Table I. In particular, when $0<g_{1\parallel}-2g_2<|g_3|$, there is a critical $\delta\mu_T$, larger than the charge-density-excitation gap, above which

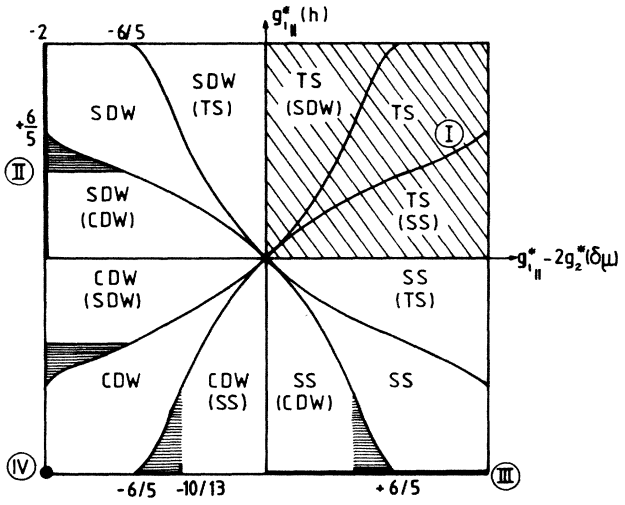

FIG. 3. Phase diagram of the 1D Fermi gas model, as a function of the fixed point coupling $g^*_{1\|}$ and $g^*_{1\|}-2g^*_2$. This diagram is straightforwardly deduced from Fig. 2. Some special values have been indicated.

superconductivity instabilities are favored at the expense of the density wave ones. In the region $\frac{3}{2}<\gamma_\sigma<2-\gamma_\rho$, the same kind of reentrant behavior as described in the preceding section can be found, namely SDW (CDW)→SDW→SDW (CDW).

D. $g_{1\|}<|g_{1\perp}|, g_{1\|}-2g_2<|g_3|$

In the absence of fields, both the ρ and σ parts of the Hamiltonian are characterized by a gap, respectively, in the spectrum of the charge and spin degrees of freedom so that the representative point of the system is given by $\gamma_\sigma=\gamma_\rho=0$. The only divergent response function is the CDW one. It must be noticed that from this point, provided the bare coupling have appropriate values (they must lie in the B region of the two parameter spaces, Fig. 1), all possible phases of the 1D Fermi gas can be reached with joint application of the two "fields," superconductivity being favored by a large $\delta\mu$ and SDW as well as TS instabilities being favored by the magnetic field.

VII. CONCLUSION

The whole parameter space, showing the different instabilities which occur with application of the two "fields" is given in Figs. 2 and 3. The obliquely-hatched area, the thick lines, and the thick points exhibit the parameter space and thus the instabilities accessible in zero "fields" ($h=0$ and $\delta\mu=0$). The effect of h and $\delta\mu$ is to translate the representative point of the system, respectively, to the top and to the right of the phase diagram (except if the bare coupling values lie in the horizontally-hatched areas). In the obliquely-hatched area (weak-coupling region), this translation is continuous as soon as h or $\delta\mu$ are nonzero. On the other hand, a "field" larger than the gap is needed to leave the thick lines or the point $\gamma_\sigma=\gamma_\rho=0$. The main instabilities are separated by the lines $\gamma_\sigma=1$ and $\gamma_\rho=1$. An infinite field moves the representative point to its bare value. Thus depending on the bare value of the couplings, different phases can be reached by variation of the fields; some of them were inaccessible when $\delta\mu=0$ and in zero magnetic field: SDW (TS), CDW (SDW), CDW (SS), and SS (TS) (Figs. 2 and 3). Figure 4 gives schematic phase diagrams as a function of the bare couplings, for different values of $\delta\mu$ and h. We have not detailed the strong-coupling region below the LE lines where the reentrant behavior described in Sec. VI B occurs. These diagrams generalize the diagram of Prigodin and Firsov[27] obtained when $G=4k_F$ and $h=0$. It must be noticed that the Fermi gas with a non-half-filled band is not identical to the case $g_3=0$. First, when $g_{1\|}-2g_2<|g_3|$, as soon as $\delta\mu$ is smaller than a critical value, the gas behavior remains that of the commensurate case. Then, even above this value, although g_3 is irrelevant, it leads to a renormalization of γ_ρ.

It must be noticed that the wave vector of the *main* instabilities is always locked at small "field." In the region (a), TS instability is dominant at wave vector $Q=0$. In the region (b), the SS instability is dominant. The wave vector Q_{SS} only depends on magnetic field and varies when $h>h_c$. In the region (c), the main instability is the SDW one; its wave vector depends only on the chemical potential and is fixed as long as $\delta\mu<\delta\mu_c$. In the strong-coupling region (d), the wave vector of the CDW depends on h and $\delta\mu$ but only above threshold values h_c and $\delta\mu_c$.

Up to this point we have been interested in the ground-state properties of the electron gas, i.e., in the response functions at vanishing frequency $\omega\to 0$. Finite temperature properties can be inferred from the above analysis. It is known, that at finite T, the renormalization trajectories stop when the energy scale reaches $\max(k_BT,\mu_BH)$ (in the spin degrees of freedom parameter space) or $\max(k_BT,\delta\mu)$. The reason is that the vertex function including, for example, $g_{1\perp}$ processes varies roughly as $\ln\max(\mu_BH,k_BT,\omega)$.[6] Then, in any case, effects described in this paper occur when $\mu_BH>k_BT$ or $\delta\mu>k_BT$.

By using the equivalence between the magnetic field and the band-filling effects on the 1D Fermi gas, we provide, although admittedly in a qualitative fashion, a complete description of the 1D electron gas under these two "fields." From Figs. 3 and 4 it is possible to predict which phase can be stabilized. The main features of this diagram are expected to give still a good description of the *quasi*-1D electron gas. In that case, it has been shown that spin effects still arise at least if $h>T_{CO}$ where T_{CO} is the 1D-3D crossover temperature and is related to the transverse coupling $t_\perp$ between chains.[7] $T_{CO}\simeq t_\perp/\pi$ in the mean field approximation for a free quasi-1D electron gas.[28,29] The observation of spin effects thus requires a compound in which the transverse integral is sufficiently small, lower than the Zeeman energy. When such is the case, we have shown that a spin-density wave can be stabilized by spin effects: this happens provided the bare values of the coupling constants are such that the SDW phase is sufficiently close in energy to the normal or superconducting state.[7] One may wonder whether such an effect could be observed in the $(TMTSF)_2X$ family. In this series, $t_\perp$ is of order 100–300 K. But Bourbonnais

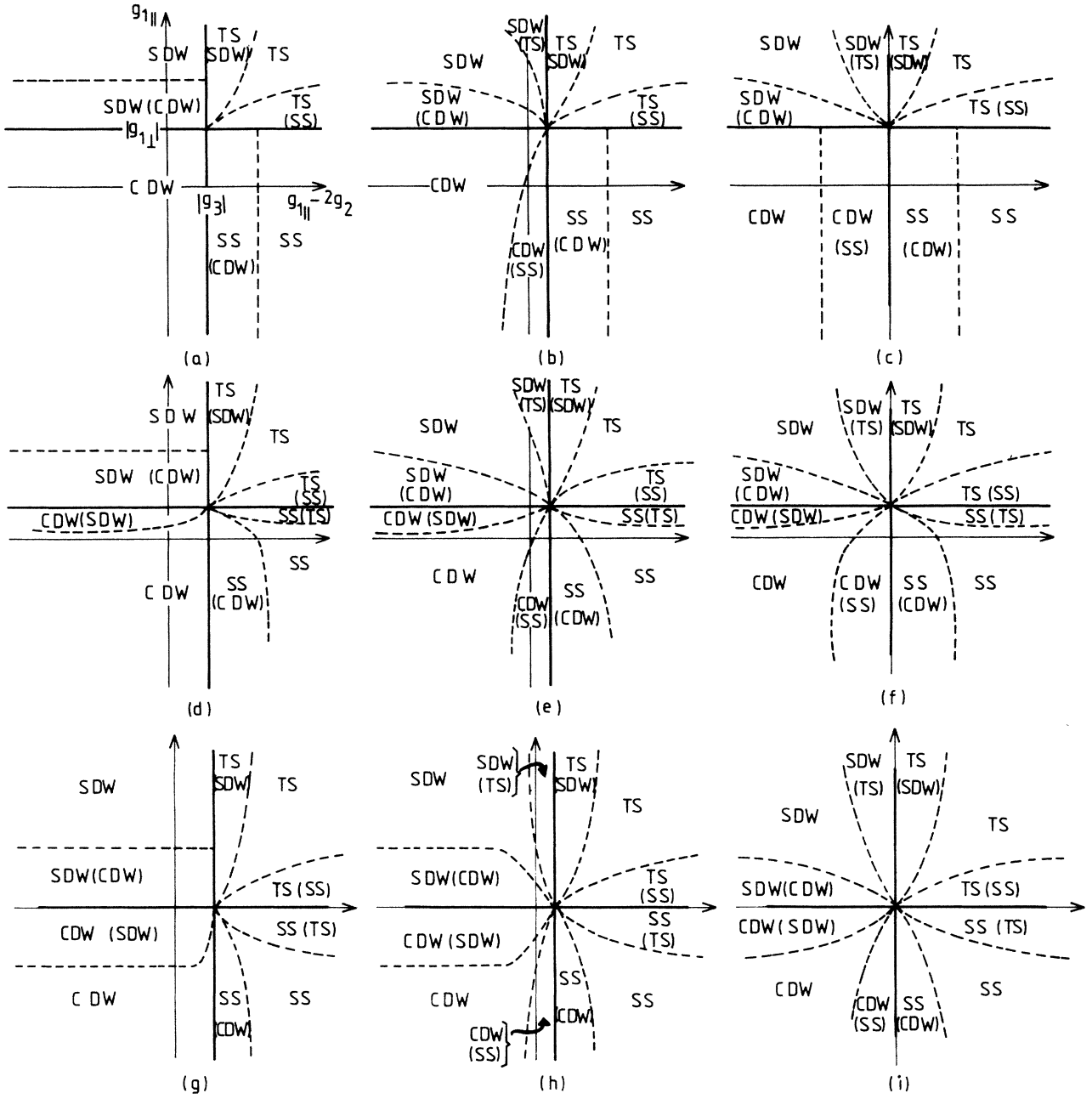

FIG. 4. Phase diagrams as a function of the bare couplings $g_{1\|}$ and $g_{1\|}-2g_2$ for different values of the fields. (a) $h=0$, $\delta\mu=0$ (Ref. 27). (b) $h=0$, $\delta\mu>\delta\mu_c$. (c) $h=0$, $\delta\mu=\infty$ (fully incommensurate case analogous to the case $g_3=0$) (Ref. 5). (d) $h>h_c$, $\delta\mu=0$. (e) $h>h_c$, $\delta\mu>\delta\mu_c$. (f) $h>h_c$, $\delta\mu=\infty$. (g) $h=\infty$, $\delta\mu=0$. (h) $h=\infty$, $\delta\mu>\delta\mu_c$. (i) $h=\infty$, $\delta\mu=\infty$. We have not detailed the regions below the LE lines where the reentrant behavior described in Sec. VI B occurs.

et al.[30] argued that the crossover temperature T_{CO} is reduced to 6—8 K by many-body effects. This allows spin effect to be relevant for fields of order 100 kG. However, such effects have not been observed up to 100 kG: the field-induced SDW phases are stabilized only by the field component along c^*. This implies either that T_{CO} is larger than 10 K or that the coupling constant values are such that spin effects are weak ones.[7] In the 3D regime, diamagnetism as well as details of the Fermi surface are essential.[2] Orbital effects suppress superconductivity above a critical field H_{c_2}, and diamagnetism has been recently shown to induce SDW phases by improving the nesting of the Fermi surface (the same mechanism could also induce a CDW).[2,31,32]

The physics seems to be simpler with regards to the charge degrees of freedom since the band filling plays the same role as the Zeeman energy on the spin degrees of freedom but there is no equivalent to orbital effects in that case. Moreover, even if T_{CO} is large, the band-filling effect on 1D fluctuations could be more accessible experi-

mentally. If $T_{CO}=30$ K, a magnetic field larger than 300 kG should be necessary to observe spin effects. And a relative variation $\delta k_F/k_F \gtrsim T_{CO}/4t_{||}$ is needed to modify the quasi-1D electron-gas stability. Typically $t_\perp = t_{||}/10$ for most of the existing quasi-1D conductors so that the required relative variation of the band filling is small and accessible experimentally. As a reminder, a relative variation of order 10% is observed in tetrathiafulvalene-tetracyanoquinodimethane (TTF-TCNQ) when pressure is varied due to the variation of charge transfer.[33] In $(TMTSF)_2X$ family the charge transfer remains complete, probably because of a large value of the Madelung energy due to a small anion-cation distance.[34]

It seems that, at the present time, the conditions for observation of spin and band-filling effects on the 1D fluctuations are not realized in the existing compounds. Necessary conditions are a small value of the crossover temperature T_{CO} (lower than 10-20 K to observe field effects), a variation of the charge transfer with pressure and temperature as for example in TTF-TCNQ, an appropriate range of coupling constants so that different phases are sufficiently close in energy (vicinity of the $g_{1||}=|g_{1\perp}|$ or $g_{1||}-2g_2=|g_3|$ lines, for example).

ACKNOWLEDGMENTS

We thank B. Horovitz and H. J. Schulz for pointing out the connection between our work and theirs on the 2D classical sine-Gordon problem of the commensurate-incommensurate transition. Discussions with H. J. Schulz are gratefully acknowledged.

[1]For a review, see *Proceedings of the International Conference on the Physics and Chemistry of Low-Dimensional Synthetic Metals, Abano-Terme, 1984* [Mol. Cryst. Liq. Cryst. **119&120**, 1 (1985)].

[2]M. Héritier, G. Montambaux, and P. Lederer, J. Phys. (Paris) Lett. **45**, L943 (1984); G. Montambaux, M. Héritier, and P. Lederer, Phys. Rev. Lett. **55**, 2078 (1985).

[3]V. J. Emery, R. Bruinsma, and S. Barišić, Phys. Rev. Lett. **48**, 1039 (1982).

[4]H. Gutfreund, B. Horovitz, and M. Weger, J. Phys. Colloq. **44**, C3-983 (1983).

[5]J. Solyom, Adv. Phys. **28**, 201 (1979).

[6]Y. A. Bychkov, L. P. Gorkov, and I. E. Dzyaloshinsky, Zh. Eksp. Teor. Fiz. **50**, 738 (1966) [Sov. Phys.—JETP **23**, 489 (1966)].

[7]G. Montambaux, M. Héritier, and P. Lederer, J. Phys. (Paris) Lett. **45**, L533 (1984).

[8]C. Seidel and V. N. Prigodin, J. Low Temp. Phys. **48**, 85 (1982).

[9]C. Seidel and V. N. Prigodin, J. Low Temp. Phys. **53**, 419 (1983).

[10]G. I. Japaridze and A. A. Nersesyan, J. Low Temp. Phys. **37**, 95 (1979).

[11]A. Luther and V. J. Emery, Phys. Rev. Lett. **33**, 589 (1974).

[12]V. J. Emery, A. Luther, and I. Peschel, Phys. Rev. B **13**, 1272 (1976).

[13]G. E. Gurgenishvili, A. Nersesyan, and L. A. Chobayan, Zh. Eksp. Teor. Fiz. **73**, 279 (1977) [Sov. Phys.—JETP **46**, 145 (1977)].

[14]R. Heidenreich, B. Schroer, R. Seiler, and D. Uhlenbrock, Phys. Lett. A **54**, 119 (1975).

[15]V. L. Pokrovsky and A. L. Talapov, Phys. Rev. Lett. **42**, 65 (1979); H. J. Schulz, Phys. Rev. B **22**, 5274 (1980); B. Horovitz, J. Phys. C **15**, 161 (1982).

[16]B. Horovitz, T. Bohr, J. M. Kosterlitz, and H. J. Schulz, Phys. Rev. B **28**, 6596 (1983).

[17]P. A. Lee, Phys. Rev. Lett. **34**, 1247 (1975).

[18]H. Gutfreund and R. A. Klemm, Phys. Rev. B **14**, 1073 (1976).

[19]A. M. Finkelstein, JETP Lett. **25**, 73 (1977).

[20]V. J. Emery, in *Highly Conducting One-Dimensional Solids*, edited by J. T. Devreese, R. P. Evrard, and V. E. Van Doren (Plenum, New York, 1979).

[21]S. T. Chui and P. A. Lee, Phys. Rev. Lett. **35**, 315 (1975).

[22]A. Luther, Phys. Rev. B **14**, 2153 (1976).

[23]H. J. Schulz, Lectures on Cooperative Phenomena at Low Dimensionality, Orsay, 1984 (unpublished).

[24]J. M. Kosterlitz, J. Phys. C **7**, 1046 (1974).

[25]A. I. Larkin and J. Sak, Phys. Rev. Lett. **39**, 1025 (1977).

[26]A. A. Ovchinnikov, Zh. Eksp. Teor. Fiz. **57**, 2137 (1969) [Sov. Phys.—JETP **30**, 1160 (1970)].

[27]V. N. Prigodin and Y. A. Firsov, Zh. Eksp. Teor. Fiz. **71**, 2252 (1976) [Sov. Phys.—JETP **44**, 1187 (1976)].

[28]S. Barišić, J. Phys. (Paris) Colloq. **44**, C3-991 (1983).

[29]V. J. Emery, J. Phys. (Paris) Colloq. **44**, C3-997 (1983).

[30]C. Bourbonnais, F. Creuzet, D. Jérome, K. Beckgaard, and A. Moradpour, J. Phys. (Paris) Lett. **45**, L755 (1984).

[31]L. P. Gor'kov and A. G. Lebed, J. Phys. (Paris) Lett. **45**, L433 (1984).

[32]K. Yamaji, Mol. Cryst. Liq. Cryst. **119**, 105 (1985).

[33]S. Megtert, R. Comès, C. Vettier, P. Pynn, and A. F. Garito, Solid State Commun. **37**, 875 (1981).

[34]C. Noguera, J. Phys. C **18**, 1647 (1985).